CFD-modelling of activated carbon fibers for indoor air purification

CFD-modelling of activated carbon fibers for indoor air purification

Jelle Roegiers [†], *Siegfried Denys*[†,*]

† Sustainable Energy, Air & Water Technology, Department of Bioscience Engineering, University of Antwerp, Groenenborgerlaan 171, B-2020 Antwerp, Belgium.

* E-mail: Siegfried.Denys@uantwerp.be

Fax: +32 3 265 32 25. Tel: +32 3 265 32 30.

Keywords

Computational Fluid Dynamics; Activated Carbon Fiber; Pressure drop; Adsorption isotherm; Breakthrough profiles

Highlights

- Pressure drop measurements for various activated carbon fiber filter thicknesses.
- CFD simulations and fitting of ACF pressure drop with Darcy-Forchheimer law.
- Investigation of three adsorption isotherms to model dynamic adsorption behavior.
- Successful Multiphysics simulation of adsorption breakthrough curves of acetaldehyde

*Corresponding author. E-mail: Siegfried.Denys@uantwerp.be

Graphical Abstract

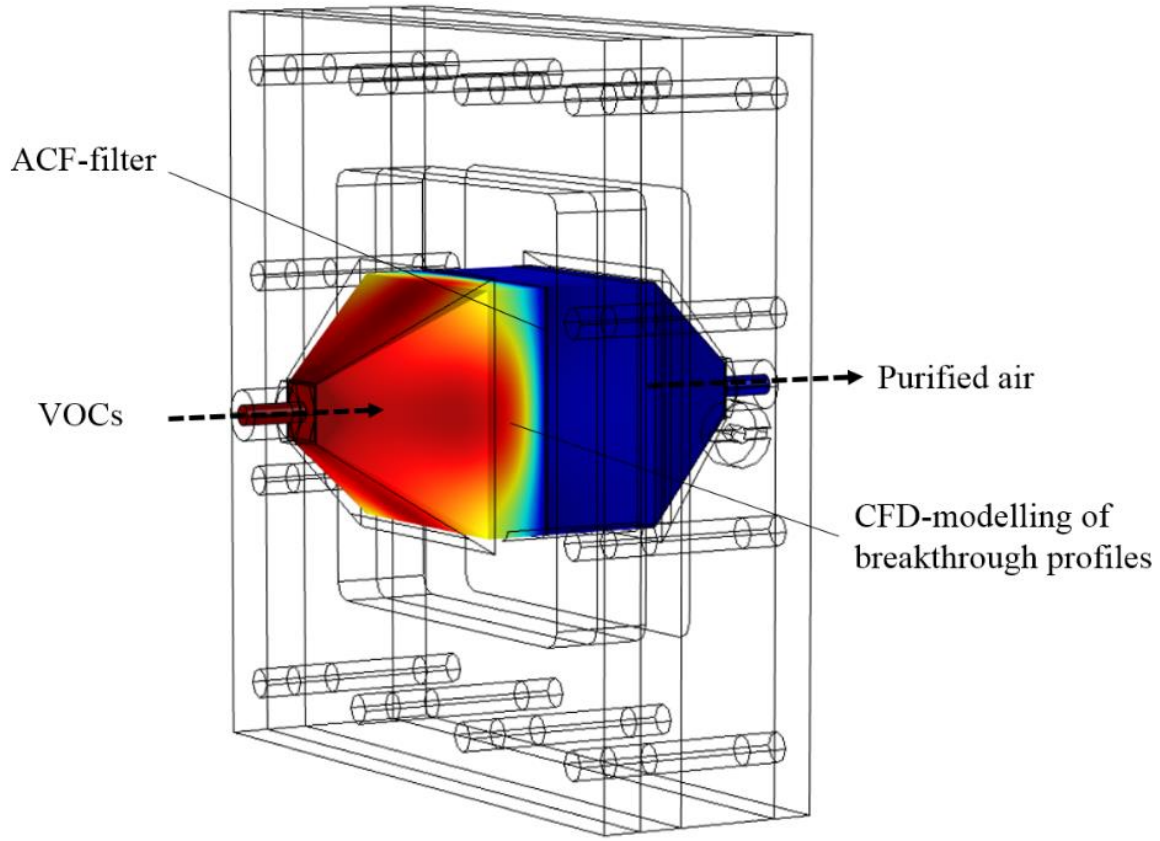

1. Abstract

Activated carbon fibers for indoor air purification were investigated by means of pressure drop and adsorption capacity. The Darcy-Forchheimer law combined with Computational Fluid Dynamics (CFD) modelling was deployed to simulate the pressure drop over an activated carbon fiber (ACF) filter with varying filter thickness. The CFD model was later combined with adsorption modelling to simulate breakthrough profiles of acetaldehyde adsorption on the ACF-filter. The adsorption model incorporates mass transfer resistance and adsorption equilibrium. It assumes local equilibrium between gas phase and solid phase. The latter was investigated for three different adsorption isotherms: linear, Langmuir and Freundlich adsorption. Successful agreement between model simulations and experimental data was obtained, using the

Freundlich adsorption model. The numerical model could provide valuable insights and allows to continuously improve the design of filtration devices.

2. Introduction

Indoor air quality has become an issue of major interest due to stringent insulation and airtightness measures in buildings [1]. Accumulation of volatile organic compounds (VOCs) can be counteracted by ventilation with outdoor air, but this demands a high energy consumption due to increased ventilation rates and conditioning of the outdoor air. Sidheswaran et al. state that a HVAC system, operating at 15-20% outdoor air and 80-85% indoor air is viable, provided that 15 to 20% of the VOCs are removed in the supply air flow [2]. Among the different strategies, activated carbon filters have been suggested as a promising approach for effective VOC removal [3–5]. Activated carbon is a widely used solution for cleaning industrial waste streams with high VOC concentrations, but recent studies have shown that activated carbon is also feasible for purification in building applications, with VOC concentrations at ppb levels [6–8]. For the same operational conditions, activated carbon fiber cloths or felts offer many advantages over conventional granular activated carbon, such as higher adsorption capacities, faster diffusion rates and kinetics, lower pressure drop, more compactness, great flexibility and easier regeneration [2,4,7,9–13]. Regeneration of activated carbon fibers can be accomplished by transmitting an electrical current, inducing the joule-effect and hence, heating the filter and desorbing the pollutants [14]. Although this technique seems very promising, there is still some investigation required to develop a commercial device for implementation in Heating, Ventilation and Air Conditioning (HVAC) systems. Integration of an ACF-filter into a HVAC system requires special features to deal with the typical high flow rates. The filter must allow the polluted air to pass through with a minimal pressure drop, but still feature sufficient adsorption capacity to effectively remove the VOCs. In this work, we investigated the pressure

drop over an activated carbon fiber cloth with varying filter thickness for typical HVAC flow rates. In addition, we developed a numerical model to validate the Darcy-Forchheimer parameters, which were calculated based on the experimental pressure curves, and to simulate the transient adsorption behavior and breakthrough curves of air contaminated with acetaldehyde, as a model compound for VOCs in indoor air. Adsorption of acetaldehyde was fitted with experimental data by three common adsorption models: Linear, Langmuir-type and Freundlich-type adsorption models. Several studies have shown that these adsorption models are valid for adsorption of volatile organic compounds on ACF filters [4,5,7,15] and some research has been conducted to model dynamic adsorption on activated carbon fibers, based on these adsorption models [7,16]. In this work, a CFD analysis is presented, combing complex fluid dynamics with adsorption kinetics to gain more valuable insights in the adsorption process. Such a model is very useful to evaluate the performance of an ACF system in unsteady operating conditions (typical for realistic applications) and can be used as a tool to develop commercial devices that can be integrated in HVAC systems [4,17,18].

3. Methodology

3.1 Pressure curves

For the development of an efficient ACF filtering device, a trade-off has to be made between the number of filter layers to increase the adsorption capacity and a maximum pressure drop for energy consumption reasons, which is evidently increased with the number of layers. It is therefore important that the filter thickness (and thus adsorption capacity) is adjusted to the (maximum) concentration of VOC in the supplying air stream. In the first part of this work, the pressure drop across an FM10 (Calgon Corp) ACF filter is studied in a closed circuit air duct system for varying thicknesses of the filter (0.5-2 mm) at typical HVAC flow rates up to 2 m/s (T=20°C, P=101.3 kPa). The FM10 woven cloth ACF filter has been studied in the past in terms

of surface density, specific surface area, apparent density, particle radius, porosity, etc. [2,7,8]. The setup consists of circular pipes with an inner diameter of 103 mm and a total length of 6m

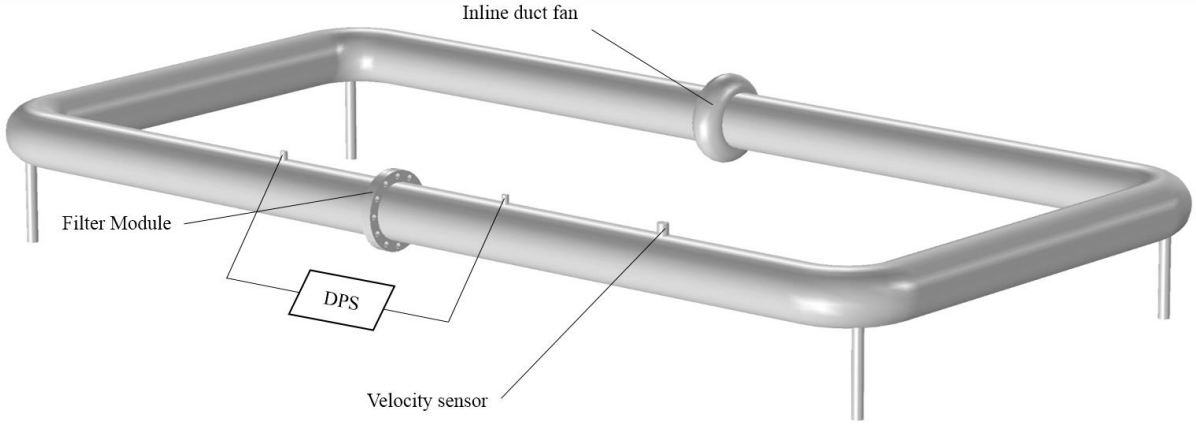

Figure 1 Closed circuit vent duct with inline duct fan, velocity sensor and differential pressure sensor (DPS)

(Figure 1). Up to four layers of ACF filter were compressed between two polylactic rings and the module was placed in line with the pipe duct. This way, the air flows perpendicular to the surface area of the filter in every experiment. The air flow rate was controlled by an inline duct fan (Ruck RS-series) with a free flow rate of 350 m^3/h and a static pressure of 250 Pa. The fan was mounted directly on the external rotor motor with controllable voltage (24V-230V) through which the air flow rate could be adjusted. The air flow rate was measured by a hotwire air velocity sensor (CTV 110, KIMO instruments) in the middle of the vent duct and the pressure drop was measured by a differential pressure sensor (DPS) consisting of a pressure module (Fluke 717 30G, Fluke Corp.) and a pressure calibrator (Fluke 700PD2, Fluke Corp.). The air flow profile was assumed to be uniform, as this was investigated earlier by Koch et al. for the same vent duct [19].

Consequently, the pressure-velocity curves were used to determine Darcy-Forchheimer parameters (eq. 1), i.e. the permeability κ (m^2) of the medium, which represents the flow resistance of the filter and the Forchheimer term β (1/m), which accounts for the non-linear behavior of the pressure difference at high flow rates due to inertial effects:

$$\frac{\Delta P}{\Delta x} = -\frac{\mu}{\kappa} v - \beta \rho v^2 \quad (1)$$

With ΔP the pressure drop (Pa), Δx de filter thickness (m), μ the dynamic viscosity of the air flow (Pa·s), ρ the density of the air flow (kg/m³) and v the air flow velocity (m/s). Since the Darcy-Forchheimer law accounts for the filter thickness Δx, the parameters κ and β are expected to be similar for every experiment. These parameters were later validated by numerical simulation with Comsol Multiphysics.

3.2 Adsorption experiments

The adsorption capacity was investigated using acetaldehyde (Messer, 1% in N_2) as a model compound for indoor air pollution. Acetaldehyde is more difficult to adsorb onto activated carbon than for example toluene due to its higher polarity, making it an ideal component to determine the minimum required adsorption capacity under given operating conditions. A filter module was developed based on the pilot unit described in Subrenat et al. (2001). The module is composed of 2 stainless steel cases, containing 2 PTFE flanges to ensure thermal and electrical insulation during the regeneration process (Figure 2). The cases were formed conically to gradually diffuse and constrict the air flow between the inlet or outlet (4 mm diameter) and the section where the carbon filter was fixed (50 × 50 mm flow-through surface). One of the PTFE flanges was equipped with two brass plate electrodes in order to provide the current for regeneration. One to four layers of carbon filter (5cm x 5cm) rested on the two electrodes, and were pressed between the two PTFE flanges. The two electrodes were externally connected to a Tenma 72-10480 DC power supply (0-30V output). The FM10 filter with the smallest thickness of 0.5mm (1 layer) was used in all adsorption experiments.

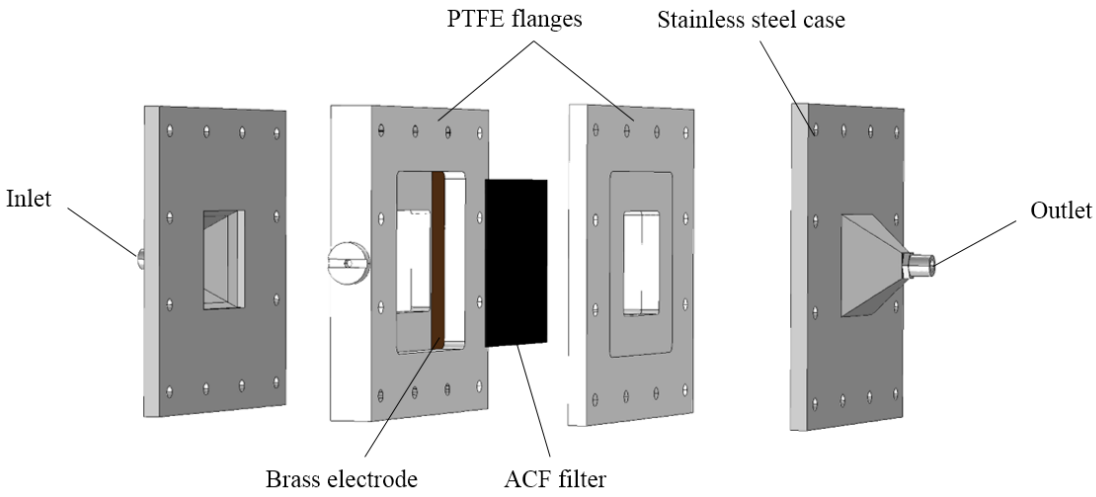

Figure 2 Configuration of the ACF-filter module with regeneration electrodes

Acetaldehyde in air was supplied to the filter module (T=20°C, P=101.2kPa) by mass flow controllers at a flow rate of 200 cm^3/min and measured at the outlet, using FTIR spectroscopy (IR peak height at 2728 cm^{-1}, which corresponds to the ν(C-H) stretch vibration [20]. The experiment continued until the breakthrough curve was complete, i.e. the outlet concentration matched the inlet concentration. The adsorbed amount of acetaldehyde at equilibrium was derived by integrating the transient acetaldehyde concentrations over the time period and subtracting the obtained value from the amount of acetaldehyde entering, a similar method was performed in previous work [21]. After each adsorption cycle, the filter was regenerated, using an electrical current and a clean air flow of 2000 cm^3/min. A constant current of 2.75 A (20V) was imposed to achieve a steady desorption temperature of 150°C due to the Joule effect, as measured with a T-type thermocouple at the surface of the filter. This temperature was persisted until acetaldehyde could not be detected anymore by the on-line FTIR measurements. Integration of the desorption curve verified that the amount of desorbed acetaldehyde equaled the amount of adsorbed acetaldehyde in the prior adsorption experiment. The breakthrough curves for 5 different inlet concentrations of acetaldehyde were studied: 1.61, 4.75, 9.74, 14.50 and 19.19 mmol/m^3 with two repetitions per concentration.

3.3 Numerical model

The Darcy-Forchheimer parameters, derived from the experimental pressure-velocity curves, were validated with Computational Fluid Dynamics. The commercial software package Comsol Multiphysics v5.3 was used for finite element modelling of the air flow through the filter medium. A straight part of the closed circuit air duct system (Figure 1) was drawn in Comsol as a simple cylindrical pipe of length 200mm, including a small section of 0.5-2mm that represented the filter medium in the pipe. The air stream was simulated as an incompressible flow with the 'Free and Porous Media Flow' physics interface in Comsol. The filter was defined as a porous medium with a porosity ϵ_p, permeability κ and Forchheimer drag β. The latter two were determined based on the pressure-velocity curves. The inlet condition was set to a uniform, normal flow velocity with the respective velocity flow rate of each experiment. A steady-state solution was obtained with a direct stationary solver, by simultaneously solving the mass continuity equation, the governing equations for the free flow (k-ε-turbulent model) and the equations for flow in porous media:

$$\rho\nabla(\mathbf{u}) = 0 \quad (2)$$

$$\rho(\mathbf{u}\cdot\nabla)\mathbf{u} = \nabla\cdot\left(-p\mathbf{I} + (\mu+\mu_T)(\nabla\mathbf{u} + (\nabla\mathbf{u})^T)\right) \quad (3)$$

$$\frac{\rho}{\epsilon_p}\left((\mathbf{u}\cdot\nabla)\frac{\mathbf{u}}{\epsilon_p}\right) = \nabla\cdot\left(-p\mathbf{I} + \frac{\mu}{\epsilon_p}(\nabla\mathbf{u} + (\nabla\mathbf{u})^T) - \frac{2\mu}{3\epsilon_p}(\nabla\cdot\mathbf{u})I\right) - (\mu\kappa^{-1} + \beta|\mathbf{u}|)\mathbf{u} \quad (4)$$

With ρ the air density (1.2041 kg/m³), $\mathbf{u}$ the velocity vector (m/s), $\mathbf{I}$ the identity matrix, p the pressure (Pa), μ the dynamic viscosity (Pa·s) and μ_T the eddy viscosity (Pa·s), which is calculated by the k-ε-model for a turbulent flow. The last term in eq. 4 represents the Darcy-Forchheimer law. In order to accurately simulate the pressure drop in the filter, a very fine swept mesh was chosen for the porous medium with 30 elements in the flow direction. The total number of mesh elements for this geometry was 188,100 with a an average quality of 0.83. The

final aim of the numerical model was to simulate the breakthrough curves of the filter with acetaldehyde as model compound. Therefore, the geometry of the filter module was constructed and meshed in Comsol. The porous medium was meshed similarly as in the previous model and the total mesh consisted of 562,400 elements (combined tetrahedral and hexahedral) with an average quality of 0.72 (Figure 3).

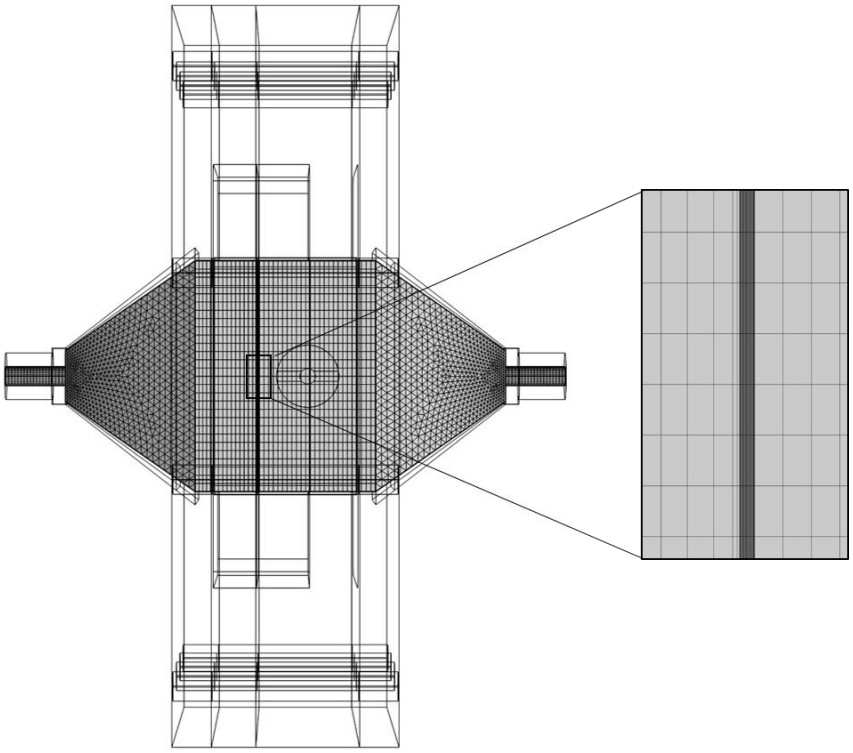

Figure 3 Mesh of the ACF-filter module

Transport of acetaldehyde in the porous medium was simulated by solving eq. 5:

$$\left(\epsilon_p + \rho_f \frac{\partial c_{ads}}{\partial c}\right)\frac{\partial c}{\partial t} + \left(c - \frac{\rho_f}{\left(1-\epsilon_p\right)} c_{ads}\right)\frac{\partial \epsilon_p}{\partial t} + \nabla \cdot (-D_e \nabla \mathrm{c}) + \mathbf{u} \cdot \nabla \mathrm{c} = 0 \qquad \mathbf{5}$$

With c the concentration of acetaldehyde (mol/m³), c_{ads} the amount of species adsorbed to the solid phase (mol/kg), ρ_f the filter density (kg/m³) and D_e the effective diffusivity within the porous matrix (m²/s). The latter is determined by:

$$D_e = \frac{\epsilon_p}{\tau} D_K = {\epsilon_p}^2 D_K \quad \textbf{6}$$

With τ the tortuosity factor, approximated by $1/\epsilon_p$, and D_K the Knudson diffusion coefficient (m^2/s) [17,22]. $\frac{\partial c_{ads}}{\partial c}$ in eq. 5 is specified by the type of adsorption isotherm. Three adsorption isotherm models were tested and validated against experimental data: Linear, Langmuir and Freundlich adsorption, respectively expressed as:

$$c_{ads} = K_{lin.} c \; ; \; \frac{\partial c_{ads}}{\partial c} = K_{lin.} \quad \textbf{7}$$

$$c_{ads} = c_{ads,max} \frac{K_{Langm.} c}{1 + K_{Langm.} c} \; ; \; \frac{\partial c_{ads}}{\partial c} = \frac{K_{Langm.} c_{ads,max}}{\left(1 + K_{Langm.} c\right)^2} \quad \textbf{8}$$

$$c_{ads} = K_{Freund.} c^{1/n} \; ; \; \frac{\partial c_{ads}}{\partial c} = \frac{1}{n} \frac{c_{ads}}{c} \quad \textbf{9}$$

Several studies have shown that Langmuir and Freundlich can effectively describe the adsorption on activated carbon material [2,6,7,9,12,15]. However, in the case of Langmuir adsorption, the expression is transformed to a linear adsorption when the concentration c (mol/m^3) is very low, i.e. $K_{Langm.} c << 1$ [15]. The Freundlich isotherm can also be approximated by a linear adsorption model when the exponent $1/n$ approaches a value of 1. The exponent $1/n$ usually ranges from 0 to 1 for most species found in indoor air [4,18]. Therefore, we tested if these assumptions are valid, so that a simple linear model can be employed to describe adsorption of acetaldehyde on the activated carbon filter. Firstly, a parameter estimation was conducted for each adsorption model, based on the adsorbed amount of acetaldehyde at equilibrium, as derived by integration of the breakthrough curves, and the inlet concentration of acetaldehyde. Secondly, the estimated parameters were deployed in the numerical model to simulate the breakthrough curves of different acetaldehyde concentrations.

4. Results and discussion

4.1 Pressure curves

Pressure curves were composed to determine the optimal filter thickness for typical HVAC flow rates. The pressure-velocity behavior at these flow rates can be represented best by the Darcy-Forchheimer law. In order to determine the Darcy-Forchheimer parameters, the data of all experiments with varying thicknesses were plotted, with the y-axis representing the ratio of pressure drop over filter thickness and the x-axis the air flow velocity (Figure 4). As seen from Figure 4, the data can be perfectly described by a polynomial expression of the second order, with a coefficient of determination of 0.995. From the quadratic regression, the permeability κ and the Forchheimer term β could be resolved, i.e. 2.71×10^{-10} m² and 64798 m^{-1} respectively.

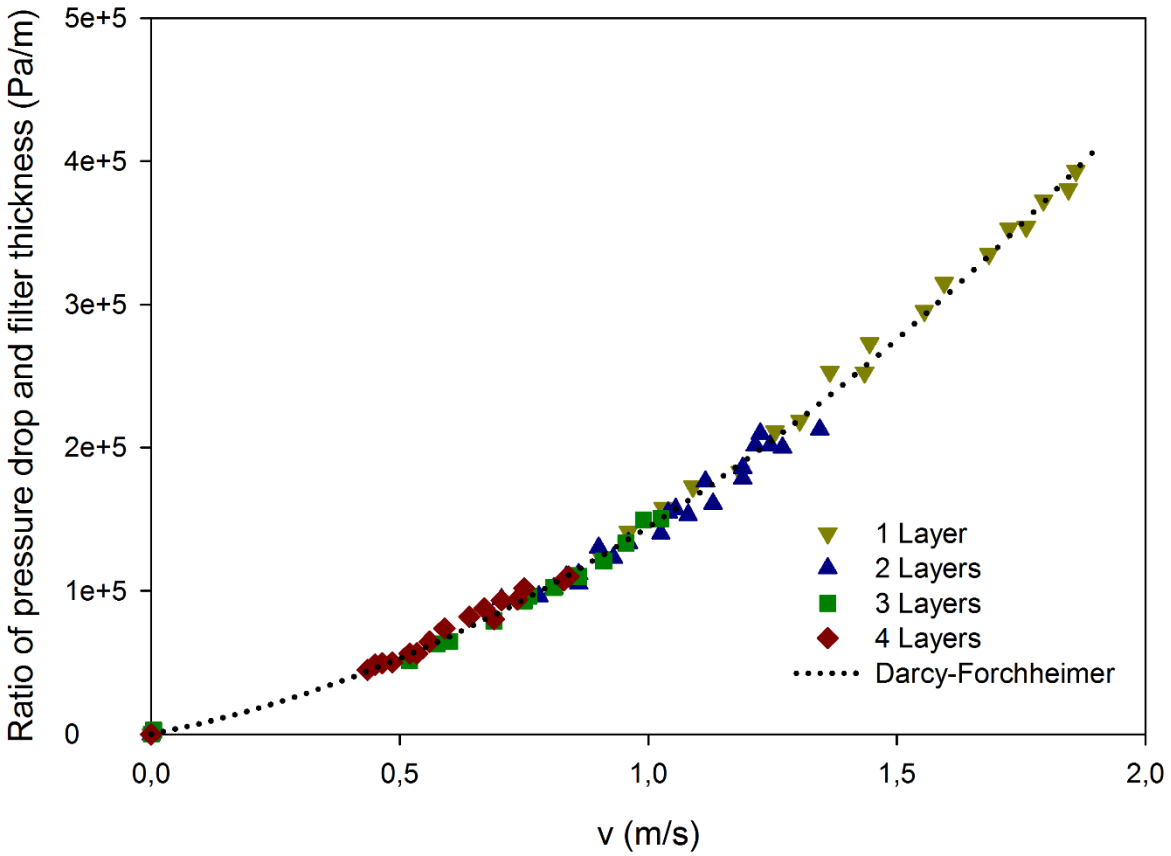

Figure 4 Ratio of pressure drop and filter thickness (Pa/m) vs air flow velocities for various filter thicknesses. (0.5-2 mm) and the fitted Darcy-Forchheimer curve

Given the fact that the coefficient of determination approximates a value of 1, it can be assumed that the Darcy-Forchheimer coefficients can be deployed to extrapolate the data to lower or higher air flow velocities. Furthermore, the pressure drop over the ACF filter can perfectly be simulated for a range of filter thicknesses while retaining the same set of parameters. In order to validate these parameters, a CFD-model was developed in which the air flow was modeled through a porous medium, with the latter representing the filter. The simulated pressure curves are shown in Figure 5.

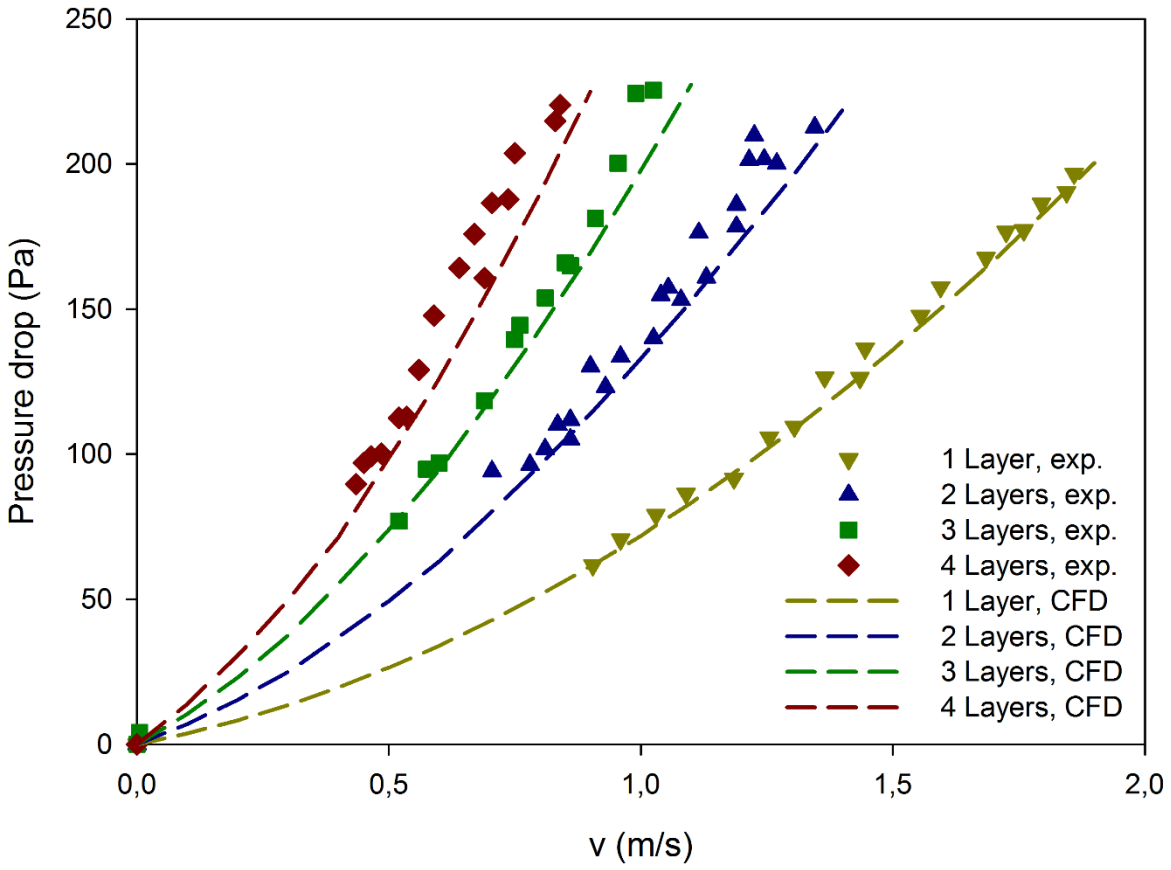

Figure 5 CFD simulations of pressure drop versus air flow for individual filter thicknesses (0.5-2mm) and validation against experimental data

The simulated pressure-velocity curves coincide well with the experimental pressure drop measurements, as emphasized by coefficients of determination of 0.989, 0.884, 0.955 and 0.817 for 1 to 4 layers of filter respectively. Therefore, Comsol Multiphysics can easily be deployed to simulate the pressure drop of a filter system at a given flow rate and for a certain system geometry and filter thickness, with the intrinsic Darcy-Forchheimer parameters.

4.2 Adsorption experiments

The breakthrough curves for 5 different acetaldehyde concentrations where determined (Figure 6). Initial breakthrough is observed almost instantaneously after the start of the experiment, due to an insufficient layer thickness of the ACF filter and the combined effect of high flow rates, ppm level concentrations, and the relatively high polarity of acetaldehyde compared to other indoor air species used in breakthrough experiments with ACF filters, such as aromatic compounds [15]. However, complete breakthrough lasted until at least 3 hours after initial breakthrough for all experiments, indicating a large adsorption capacity for acetaldehyde. By integrating these adsorption curves, the adsorbed amount of acetaldehyde at equilibrium could be determined. From this, the adsorption isotherm (at T=20°C), i.e. the adsorbed amount of acetaldehyde vs. inlet concentration, could be derived (Figure 7). Although the breakthrough curves for the repetitive experiments aligned, there was still an uncertainty on the inlet concentration of acetaldehyde, limited by the mass flow controllers. This effected integration of the breakthrough curves, as presented by the error bars on Figure 7.

1

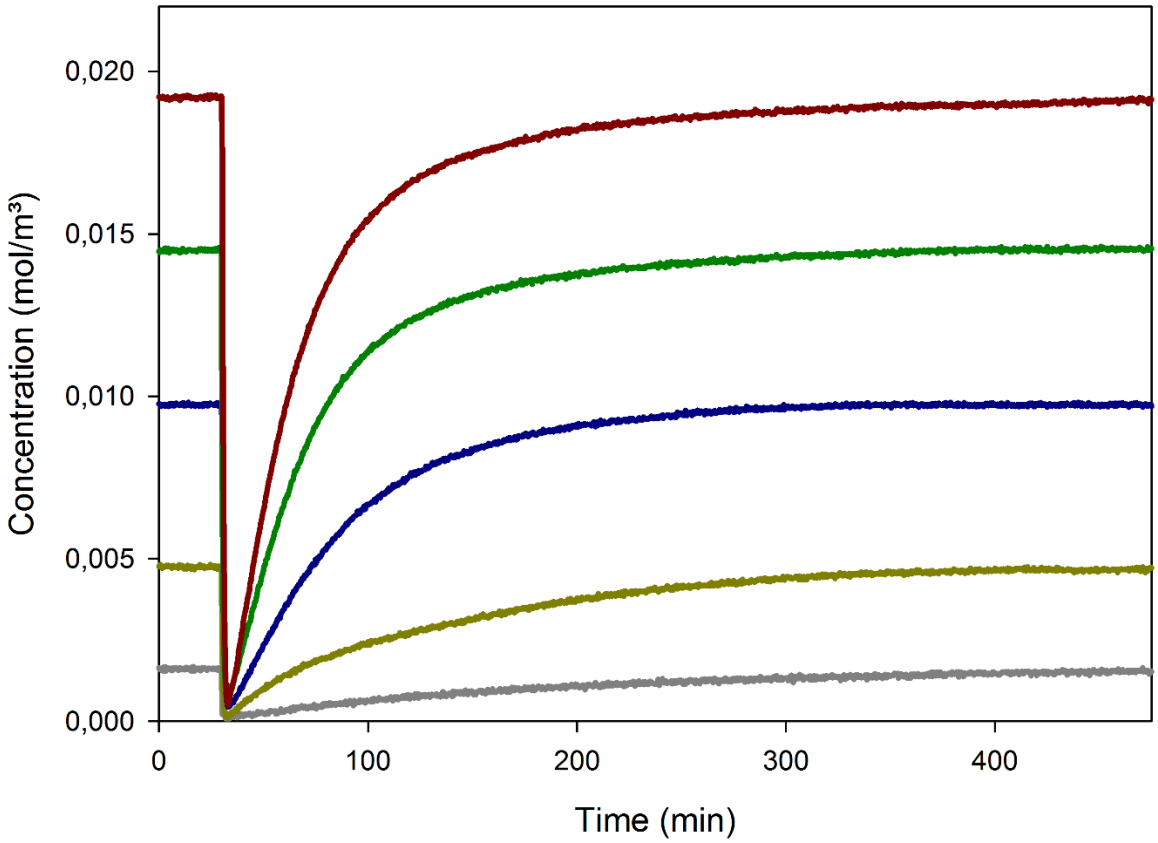

Figure 6 Breakthrough profiles for 5 different acetaldehyde inlet concentrations

2

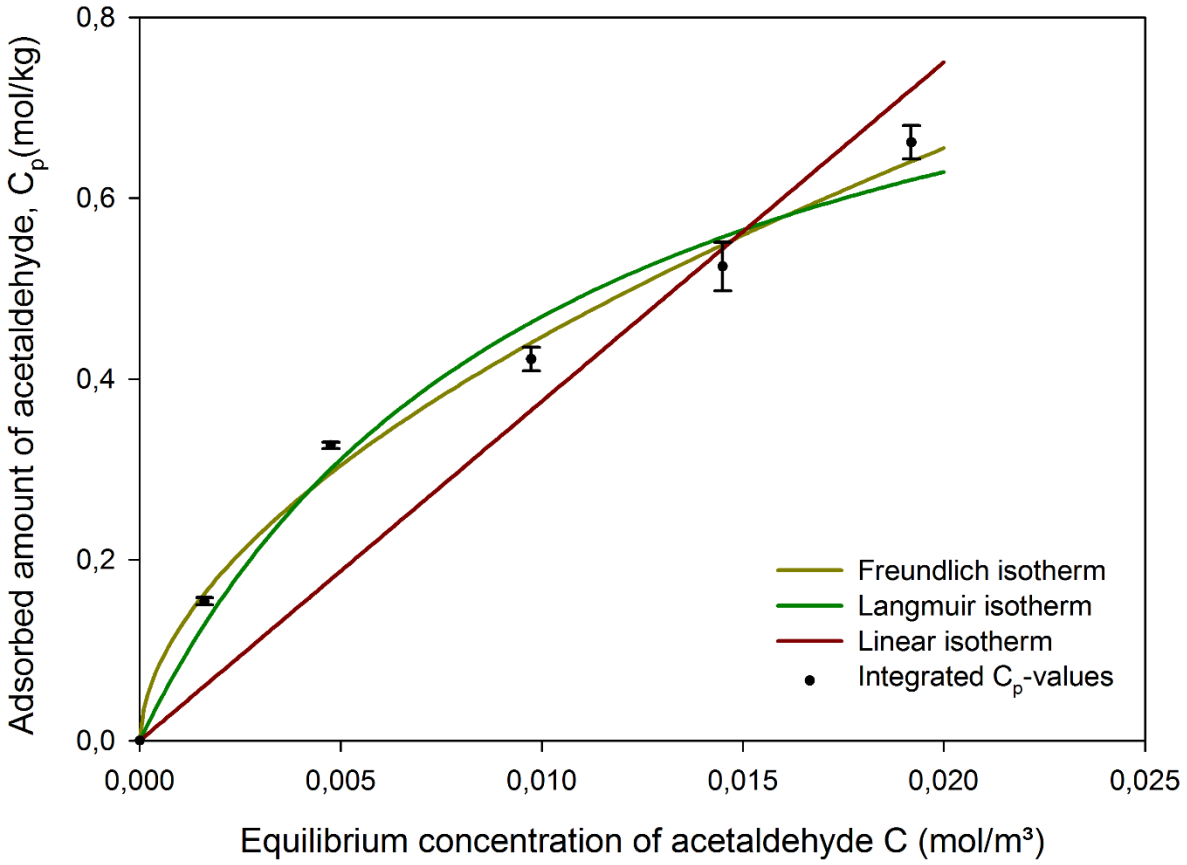

Figure 7 Freundlich, Langmuir and linear isotherms fitted with experimentally determined, adsorbed amount of acetaldehyde

The Langmuir, Freundlich and linear adsorption models could be fitted with the experimental integrated c_{ads}-values with coefficients of determination of 0.980, 0.992 and 0.872 respectively. The resulting parameters are listed in Table 1. Cal et al. (1994) reported values for similar pollutants of 0.142-0.580 and 2.81-117 (mol/kg)/(mol/m³)$^{(1/n)}$ for 1/n and $K_{Freund.}$ respectively [4]. Yao et al. (2009) fitted the Freundlich equation for 27 different indoor air species, resulting in values ranging from 0.072 to 0.821 for 1/n and 0.1 to 7.84 (mol/kg)/(mol/m³)$^{(1/n)}$ for $K_{Freund.}$ [18]. Brasquet & Le Cloirec (1997) and Popescu et al. (2013) both reported Langmuir parameters for several VOCs ranging from 2.12 to 13.84 mol/kg for $c_{ads,max}$ and 6.44-15000 m³/mol for $K_{Langm.}$ [5,15]. Thus, the obtained parameters coincide well with findings in earlier studies for similar volatile organic compounds in the same range of pollutant concentrations.

Table 1 Equilibrium parameters

Parameter	Value
Linear	
$K_{lin.}$ (m³/kg)	37.52
Langmuir	
$c_{ads,max}$ (mol/kg)	0.95
$K_{Langm.}$ (m³/mol)	96.65
Freundlich	
$1/n$ (-)	0.55
$K_{Freund.}$ (mol/kg)/(mol/m³)$^{(1/n)}$	5.71

4.3 Numerical model

Comsol Multiphysics was also used to simulate the breakthrough curves of acetaldehyde in the filter module. Firstly, the air flow through the filter module was simulated, based on the earlier determined Darcy-Forchheimer parameters, at a flow rate of 200 cm³/min. Figure 8 shows that the airflow is uniformly distributed, utilizing the complete filter surface area. However, it should be noted that the high inflow velocity resulted in a concentrated air flow, impacting the filter surface. A more uniform air inflow is desired and should be taken in consideration for upscale purposes. Based on these fluid flow characteristics and the adsorption models with their respective estimated adsorption parameters, the breakthrough curves were simulated for 5 different inlet concentrations and validated against the experimental results.

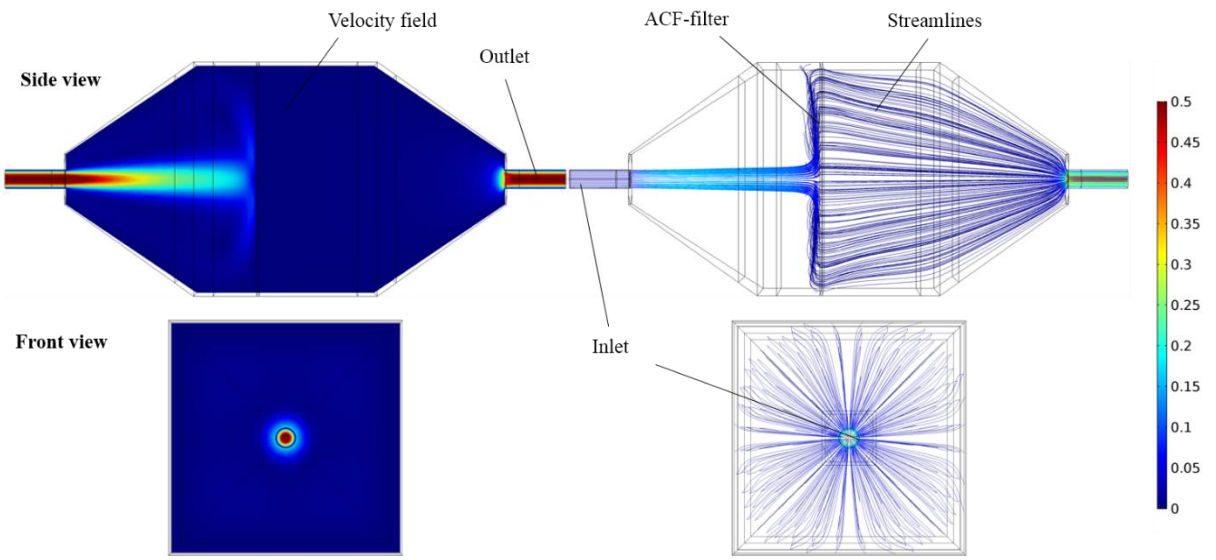

Figure 8 Fluid flow dynamics (air flow velocity, m/s) inside the ACF-filter module for an airflow rate of 200 cm³/min and 0.5 mm filter thickness (1 layer)

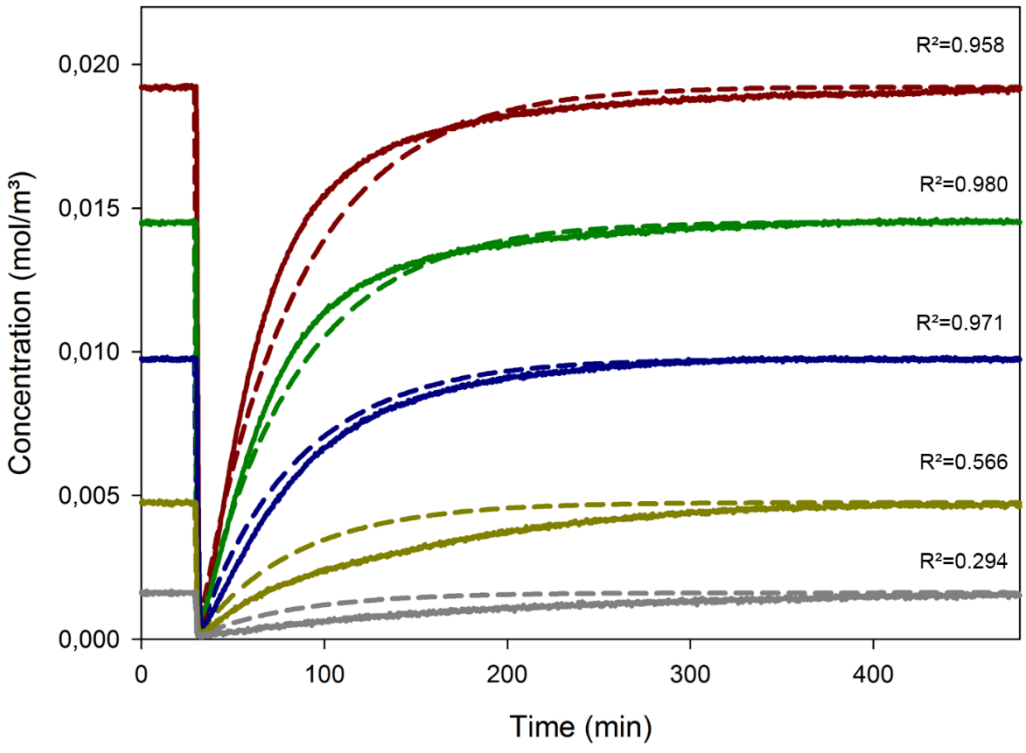

Figure 9 Simulated breakthrough profiles with linear isotherm (dashed) vs experimental data (continuous)

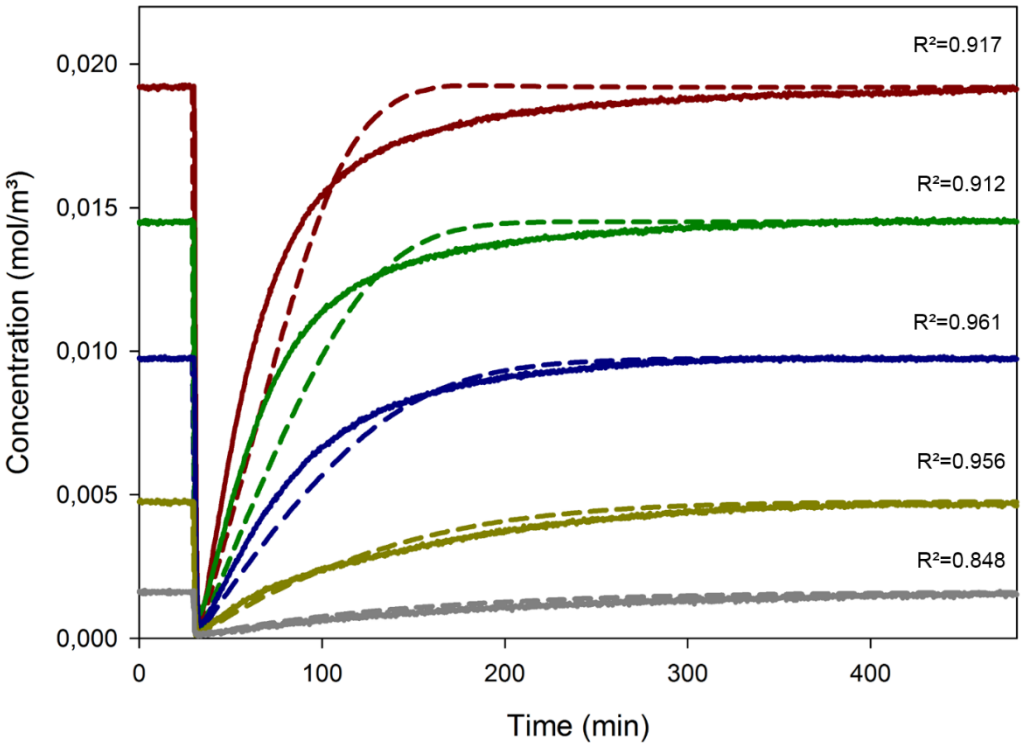

Figure 10 Simulated breakthrough profiles with Langmuir isotherm (dashed) vs experimental data (continuous)

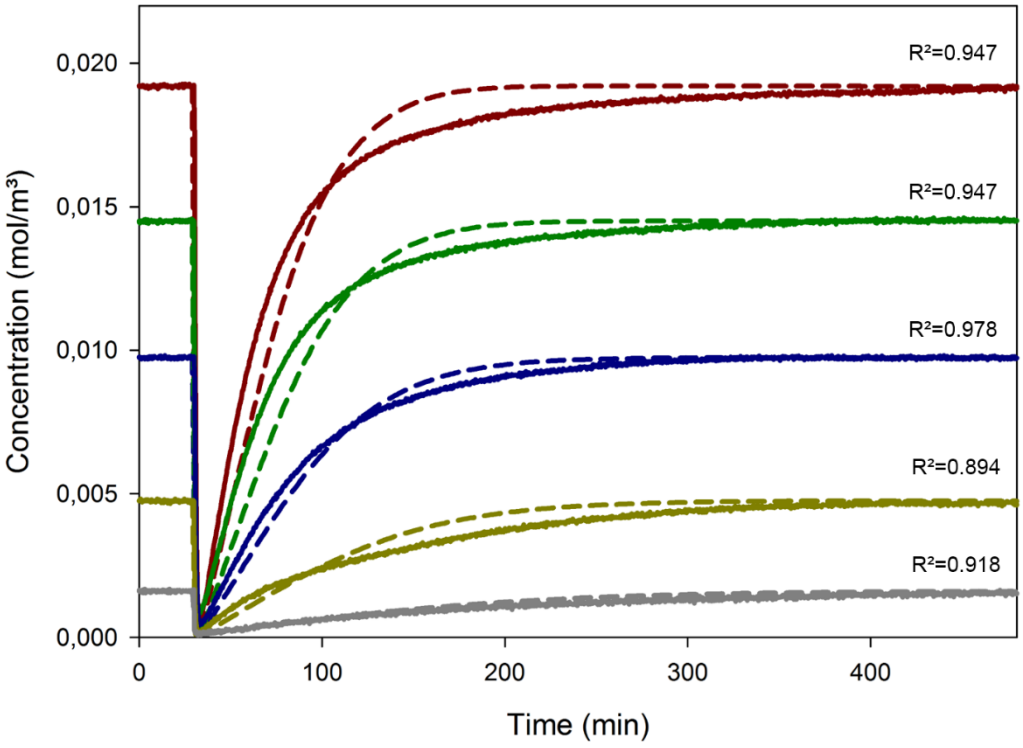

Figure 11 Simulated breakthrough profiles with Freundlich isotherm (dashed) vs experimental data (continuous)

Each adsorption model has been assessed by comparing the measured and simulated breakthrough curves, as shown in Figure 9 to Figure 11. In a first observation, it can be concluded that the Freundlich adsorption model shows the best overall fit. Secondly, the three adsorption models deliver significantly different breakthrough curves, as emphasized by the distinct coefficients of determination. This can be explained by that fact that under dynamic conditions, the gas phase inside the porous medium may present values that range from 0 to equilibrium concentration due to mass transfer resistance, resulting in different transient adsorption curves [22]. Since the model assumes thermodynamic equilibrium, adsorption occurs instantaneously based on the local concentration and the specific isotherm model. Including kinetics for adsorption/desorption processes in future work could improve the simulated breakthrough curves, as we have shown in previous modelling work [21]. This could clarify the relatively poor fit of Langmuir isotherm simulations for higher inlet concentrations. The linear model data presents an opposite trend, showing good agreement for higher acetaldehyde concentrations, but more rapid breakthrough than the experimental data for the lower inlet concentrations. This could be expected, based on the linear isotherm in Figure 7, indicating that the linear adsorption model should only be deployed in very small ranges of equilibrium concentrations. Despite the best fit for the Freundlich model, the simulated data could not perfectly align with the measured breakthrough curves. The error-level on the c_{ads}-values, integrated from the experimental data, will certainly play a role in this and optimization of the adsorption parameters could further improve the model. However, the main reason for the deviation of the simulated breakthrough curve is possibly due to the influence of intraparticular resistance on the mass transfer kinetics. Several studies show that intraparticle mass transfer is the limiting step of the adsorption kinetics, while distinguishing between pore diffusion, as defined by the effective diffusion coefficient, and surface diffusion [16,17,22,23]. The latter becomes increasingly important with a higher microporous volume, as can be the

case for activated carbon fiber filters. Unfortunately, Comsol Multiphysics v5.3 does not provide an option to include surface diffusion in the governing equations, so that mass transfer inside the pores can only be expressed by pore volume diffusion. Moreover, it could be interesting, to assess alternative adsorption isotherms in future research. For example the empirical Dubinin-Radushkevich isotherm model, which is used to describe adsorption of subcritical vapors onto microporous solids such as activated carbon or zeolites [24,25]. Additionally, better fittings with experimental data could be achieved by isotherm models which combine both Langmuir and Freundlich expressions, such as Sips or Koble-Corrigan isotherm models [24] or the Toth model, which is an improvement to the Langmuir isotherm model [24,26,27]. Nevertheless, the developed model has proven acceptable performance, given the complex dynamic behavior of the system, and it can provide valuable insights such as spatial variation in saturation level of the level, as shown in Figure 12.

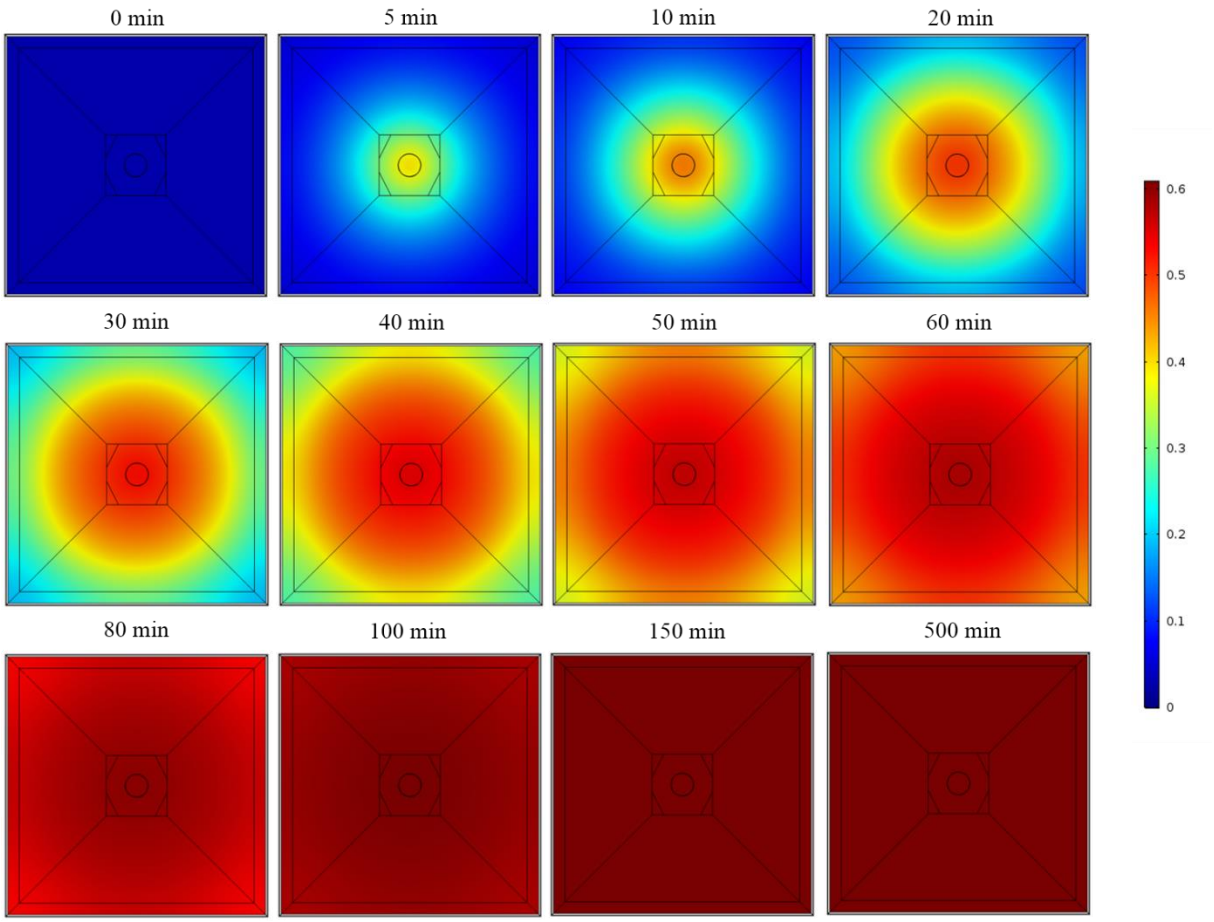

Figure 12 Spatial variation of adsorbed acetaldehyde (mol/kg) on the ACF filter (as seen from the inlet) at different time intervals (min); simulated with the Freundlich model.

It can be seen that the dynamics of the fluid flow greatly influences the spatial saturation of the ACF filter. Saturation starts in the center of the filter, due to the high inlet velocity, and spreads towards the edges of the filter later in the adsorption process. The saturation process can directly be linked to the breakthrough curves in Figures 9 to 11. The steep drop in the breakthrough curves results from a rapid adsorption in the center of the filter, followed by rapid increase in the outlet concentration of the filter module. After 1 hour, the curves begin to flatten out towards equilibrium concentration. This is reflected by the mere change in saturation level after 1 hour as seen in Figure 12, i.e. a color change from light red to dark red. Based on the spatial variation of adsorbed acetaldehyde combined with fluid flow dynamics, the geometry of the filter module can be adapted and optimized in the numerical model to achieve a more uniform level

of saturation during the operating time of the filter and hence, a better control over the breakthrough curves.

5. Conclusions

The pressure drop over an ACF-filter can be described with the Darcy-Forchheimer law with unique parameter values for various filter thicknesses. The parameters were determined by quadratic regression, using pressure-velocity measurements in a closed circuit vent duct. CFD-modelling has successfully demonstrated the validity of the Darcy-Forchheimer parameters. Consequently, the CFD model was extended to simulate the breakthrough profile of acetaldehyde adsorption on the ACF-filter. Three adsorption isotherm models were investigated: Linear, Langmuir and Freundlich adsorption. The Freundlich model has proven the most suitable fit with experimental breakthrough profiles for different inlet concentrations of acetaldehyde. However, there is still some room for improvement by including surface diffusion as a mass transfer mechanism inside the pore system, combined with effective pore diffusion. In this work, only the latter could be included due to practical limitations. Nonetheless, the numerical model was able to generate a good agreement with experimental data and could provide valuable insights. Continuous improvement of the numerical model will speed up the development of commercial ACF devices for indoor air purification.

6. Appendix

c	$Concentration\ (mol/m^3)$
c_{ads}	$Amount\ of\ adsorbed\ acetaldehyde\ (mol/kg)$
$c_{ads,max}$	$Maximum\ amount\ amount\ of\ adsorbed\ acetaldehyde\ (mol/kg)$
D_e	$Effective\ diffusivity\ (m^2/s)$
D_K	$Knudson\ diffusion\ coefficient\ [m^2/s]$
I	$Identity\ matrix$
$K_{Freund.}$	$Freundlich\ equilibrium\ constant\ (mol/kg)/(m^3/mol)^n$
$K_{Langm.}$	$Langmuir\ equilibrium\ constant\ (m^3/mol)$
$K_{lin.}$	$Linear\ equilibrium\ constant\ (m^3/kg)$
$1/n$	$Freundlich\ exponent\ (-)$
P	$Pressure\ (Pa)$
v	$Velocity\ (m/s)$
x	$Filter\ thickness\ (m)$
β	$Forchheimer\ term\ (1/m)$
ϵ_p	$Porosity\ (-)$
κ	$Permeability\ (m^2)$
μ	$Dynamic\ viscosity\ [Pa \cdot s]$
μ_T	$Eddy\ viscosity\ [Pa \cdot s]$
ρ	$Density\ [kg/m^3]$
τ	$Tortuosity\ (-)$

7. References

[1] R. Kostiainen, Volatile organic compounds in the indoor air of normal and sick houses, Atmos. Environ. 29 (1995) 693–702. doi:10.1016/1352-2310(94)00309-9.

[2] M.A. Sidheswaran, H. Destaillats, D.P. Sullivan, S. Cohn, W.J. Fisk, Energy efficient indoor VOC air cleaning with activated carbon fiber (ACF) filters, Build. Environ. 47 (2012) 357–367. doi:10.1016/j.buildenv.2011.07.002.

[3] K.L. Foster, R.G. Fuerman, J. Economy, S.M. Larson, M.J. Rood, Adsorption characteristics of trace volatile organic compounds in gas streams onto activated carbon fibers, Chem. Mater. 4 (1992) 1068–1073. doi:10.1021/cm00023a026.

[4] M.P. Cal, S.M. Larson, M.J. Rood, Experimental and modeled results describing the adsorption of acetone and benzene onto activated carbon fibers, Environ. Prog. 13 (1994) 26–30. doi:10.1002/ep.670130114.

[5] C. Brasquet, P. Le Cloirec, Adsorption onto activated carbon fibers: Application to water and air treatments, Carbon N. Y. 35 (1997) 1307–1313. doi:10.1016/S0008-6223(97)00079-1.

[6] M. Yao, Q. Zhang, D.W. Hand, D.L. Perram, R. Taylor, Investigation of the treatability of the primary indoor volatile organic compounds on activated carbon fiber cloths at typical indoor concentrations, J. Air Waste Manag. Assoc. (2009). doi:10.3155/1047-3289.59.7.882.

[7] M. Yao, Q. Zhang, D.W. Hand, R. Taylor, Modeling of Adsorption and Regeneration of Volatile Organic Compounds on Activated Carbon Fiber Cloth, J. Environ. Eng. 135 (2009) 31–36. doi:10.1061/(ASCE)EE.1943-7870.0000110.

[8] M. Yao, Q. Zhang, D.W. Hand, D. Perram, R. Taylor, Adsorption and regeneration on

activated carbon fiber cloth for volatile organic compounds at indoor concentration levels, J. Air Waste Manag. Assoc. 59 (2009) 31–36. doi:10.3155/1047-3289.59.1.31.

[9] C. Lorimier, A. Subrenat, L. Le Coq, P. Le Cloirec, Adsorption of toluene onto activated carbon fibre cloths and felts: Application to indoor air treatment, Environ. Technol. 26 (2005) 1217–1230. doi:10.1080/09593332608618600.

[10] A. Badalyan, R. Bromball, P. Pendleton, W. Skinner, An assessment of activated carbon cloth microporosity change due to chemical activation, Carbon N. Y. 48 (2010) 1004–1011. doi:10.1016/j.carbon.2009.11.019.

[11] M. Suzuki, Activated carbon fiber: Fundamentals and applications, Elsevier Sci. Ltd. 32 (1993) 577–586. doi:10.1016/0008-6223(94)90075-2.

[12] P. Le Cloirec, Adsorption onto activated carbon fiber cloth and electrothermal desorption of volatile organic compound (VOCs): A specific review, Chinese J. Chem. Eng. (2012). doi:10.1016/S1004-9541(11)60207-3.

[13] D. Das, V. Gaur, N. Verma, Removal of volatile organic compound by activated carbon fiber, Carbon N. Y. 42 (2004) 2949–2962. doi:10.1016/j.carbon.2004.07.008.

[14] A. Subrenat, J.N. Baléo, P. Le Cloirec, P.E. Blanc, Electrical behaviour of activated carbon cloth heated by the joule effect: Desorption application, Carbon N. Y. 39 (2001) 707–716. doi:10.1016/S0008-6223(00)00177-9.

[15] R.S. Popescu, P. Blondeau, E. Jouandon, J.C. Costes, J.L. Fanlo, Elemental modeling of adsorption filter efficiency for indoor air quality applications, Build. Environ. 66 (2013) 11–22. doi:10.1016/j.buildenv.2013.01.025.

[16] L. Fournel, P. Mocho, R. Brown, P. Le Cloirec, Modeling breakthrough curves of volatile organic compounds on activated carbon fibers, Adsorption. 16 (2010) 147–153. doi:10.1007/s10450-010-9207-4.

[17] M. Lordgooei, M.J. Rood, M. Rostam-Abadi, Modeling effective diffusivity of volatile organic compounds in activated carbon fiber, Environ. Sci. Technol. 35 (2001) 613–619. doi:10.1021/es0012568.

[18] M. Yao, Q. Zhang, D.W. Hand, D.L. Perram, R. Taylor, Investigation of the treatability of the primary indoor volatile organic compounds on activated carbon fiber cloths at typical indoor concentrations, J. Air Waste Manag. Assoc. 59 (2009) 882–890. doi:10.3155/1047-3289.59.7.882.

[19] K. Koch, R. Samson, S. Denys, Aerodynamic characterisation of green wall vegetation based on plant morphology: An experimental and computational fluid dynamics approach, Biosyst. Eng. (2019). doi:10.1016/j.biosystemseng.2018.10.019.

[20] T. Tytgat, B. Hauchecorne, M. Smits, S.W. Verbruggen, S. Lenaerts, Concept and validation of a fully automated photocatalytic test setup., J. Lab. Autom. 17 (2012) 134–43. doi:10.1177/2211068211424554.

[21] J. van Walsem, S.W. Verbruggen, B. Modde, S. Lenaerts, S. Denys, CFD investigation of a multi-tube photocatalytic reactor in non-steady-state conditions, Chem. Eng. J. 304 (2016) 808–816. doi:10.1016/j.cej.2016.07.028.

[22] G. Marbán, T. Valdés-Solís, A.B. Fuertes, Modeling the breakthrough behavior of an activated carbon fiber monolith in n-butane adsorption from diluted streams, Chem. Eng. Sci. 61 (2006) 4762–4772. doi:10.1016/j.ces.2006.03.008.

[23] T. Cheng, Y. Jiang, Y. Zhang, S. Liu, Prediction of breakthrough curves for adsorption on activated carbon fibers in a fixed bed, Carbon N. Y. 42 (2004) 3081–3085. doi:10.1016/j.carbon.2004.07.021.

[24] K.Y. Foo, B.H. Hameed, Insights into the modeling of adsorption isotherm systems, Chem. Eng. J. (2010). doi:10.1016/j.cej.2009.09.013.

[25] C. Nguyen, D.D. Do, The Dubinin-Radushkevich equation and the underlying microscopic adsorption description, Carbon N. Y. (2001). doi:10.1016/S0008-6223(00)00265-7.

[26] M.A. Lillo-Ródenas, D. Cazorla-Amorós, A. Linares-Solano, Benzene and toluene adsorption at low concentration on activated carbon fibres, Adsorption. (2011). doi:10.1007/s10450-010-9301-7.

[27] R.S. Juang, F.C. Wu, R.L. Tseng, Adsorption isotherms of phenolic compounds from aqueous solutions onto activated carbon fibers, J. Chem. Eng. Data. (1996). doi:10.1021/je950238g.